JOURNAL OF MATERIALS SCIENCE 41 (2006) 97–106

Magnetoelectric coupling, efficiency, and voltage gain effect in piezoelectric-piezomagnetic laminate composites

SHUXIANG DONG, JIE-FANG LI, D. VIEHLAND
Department of Materials Science & Engineering, Virginia Tech, Blacksburg, VA 24061

The magnetoelectric (ME) effect of piezoelectric-magnetostrictive laminate composites, which is a product tensor, has been studied. Based on piezoelectric and piezomagnetic constituent equations, the longitudinal-mode vibration and equivalent circuits have been derived. The effective magnetoelectric coupling coefficient, voltage-gain, and output efficiency have been determined. Our results show: (i) that there is an extreme high voltage gain effect of >260 under resonance drive: the induced ME voltage is much higher than the input voltage to the coils for magnetic excitation; (ii) that there is an optimum ratio of the piezoelectric to piezomagnetic layer thicknesses, which results in maximum effective magnetoelectric coupling; and (iii) that the maximum output efficiency of magnetoelectric laminate at resonance drive is ~98%, if eddy currents are neglected. This high ME voltage gain effect offers potential for power transformer applications.

1. Introduction

The magnetoelectric effect is a polarization response to an applied magnetic field H, or conversely a spin response to an applied electric field E [1]. Ferroelectromagnetic materials have been studied [2–5] such as $BiFeO_3$ and $Pb(Fe_{1/2}Nb_{1/2})O_3$; however to date, a single phase material with a high inherent coupling between spin and polarization has yet to be found.

Magneto-electric behavior has also been studied as a composite effect in multi-phase systems consisting of both piezoelectric and magnetostrictive materials [6–32]. Piezoelectric/ magnetostrictive composites have been the topic of numerous investigations, both experimentally and analytically. Various composite connectivities of the two phases have been studied including: 3-3 (i.e., ceramic-ceramic particle composite [6, 7]; ceramic, rare-earth iron alloys and polymer composites [8, 9]) and 2-2 (laminate composites [10–32]). These studies have confirmed the existence of magnetoelectric effects in composites; however, the magnitude of the coupling was low for both connectivities.

Analytical and experimental investigations have focused on 2-2 type laminate composites of magnetostrictive/piezoelectric bi-materials operated at both low and resonance frequency ranges [9–17]. Recently, we have designed and prototyped several resonance-type laminate geometries, and a strong resonance ME effect and ME voltage gain effect were observed [11, 15–17]. Resonance-type magnetoelectric devices are needed in applications as high-power solid-state devices. Such applications require high voltage gains and high output efficiencies. In this paper, we will further treat the resonance ME effect using an analytical approach. Our approach is based on an equation of motion to couple the two constitutive equations of the piezoelectric and piezomagnetic bi-materials, and an equivalent circuit method. This method is significantly different than prior analytical method [8,17–19, 22, 23]. Our analysis was developed for a long-plate-type magnetostrictive/piezoelectric laminate, operated in a longitudinal-mode vibration. The purpose was to extend the analytical approach for a resonance type ME transformer. The effective ME coupling coefficient, voltage gain, and output efficiency at resonance have been derived. The results show the presence of extremely high magnetoelectric voltage gain effects, suitable for solid-state transformer applications.

2. Analysis of Piezoelectric-magnetostrictive laminate composites under longitudinal excitation

Fig. 1 shows the schematic of the composite geometry used in this investigation. It is a long plate type

0022-2461
DOI: 10.1007/s10853-005-5930-8

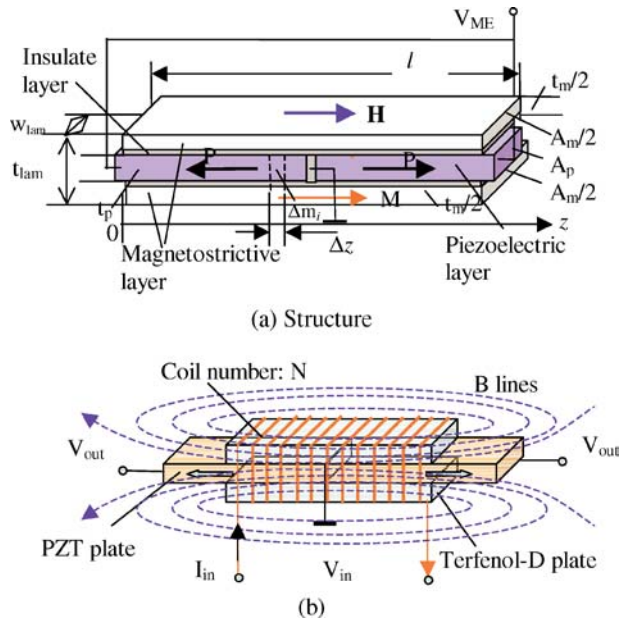

Figure 1 (a) Schematic of the geometry of the magnetostrictive/piezoelectric laminate composite, the polarization direction of the two piezoelectric plates is along the longitudinal direction, the magnetic field is applied along longitudinal direction; and (b) schematic and operational principle of the ME transformer. An N-turn coil carrying current I_{in} around the magnetoelectric laminate is used to produce a magnetizing field.

piezoelectric/magnetostrictive laminate composite, in which the piezoelectric layer (PZT) is sandwiched between two magnetostrictive ones (Terfenol-D, $Tb_{1-x}Dy_xFe_{2-y}$). More complicated geometries of this general type, such as a thin multi-layer type, are possible, but that given in Fig. 1a readily allows for equivalent circuit analysis. Conductive magnetostrictive layers are separated from a piezoelectric one by thin insulating layers. Thus, eddy currents are effectively eliminated. This long-type ME laminate design intensifies the longitudinal direction vibrations along which fields are applied. The two piezoelectric layers are longitudinally polarized reversely (push-pull type [11]), which maximizes the voltage and power outputs.

The working principle is as follows. A harmonic ac magnetic field H is applied along the longitudinal direction of the composite. This causes the two magnetostrictive layers to shrink/expand in response to H. The magnetostrictive strain acts upon the piezoelectric layer that is bonded between the two magnetostrictive layers, causing the piezoelectric layer to strain, producing a voltage output. This transduction of magnetic to electrical energy is what we designate as the magnetoelectric coupling effect.

A solenoid with N turns around the laminate that carries a current of I_{mag} (or I_{in}) was used to excite an ac magnetic field H_{ac}, as shown in Fig. 1b. An input ac voltage applied to the coils was V_{mag} (or V_{in}), and its frequency was f. This excites a H_{ac} of the same frequency f, along the longitudinal direction of the laminate. When the frequency of H_{ac} is equal to the resonance frequency of the laminate, the magnetoelectric coupling effect is so strong that the output ME voltage V_{out} induced in the piezoelectric layer is much higher than V_{mag}. Thus, under resonant drive, there is a high voltage gain, due to the magnetoelectric effect.

To obtain a maximum magnetoelectric voltage gain, the polarization direction of the piezoelectric layer was chosen to be along its length direction under longitudinal vibration, as shown in Fig. 1a. This is because both the piezoelectric constant g_{33} and electromechanical coupling coefficient k_{33} in the longitudinal mode are 2× that of the transverse g_{31} and k_{31} coefficients [33]. Consequently, higher output voltages V_{out} can be obtained from the magnetoelectric laminate. Magnetostrictive Terfenol-D also has the highest coupling in the longitudinal mode [34]. Thus, to obtain the maximum magnetoelectric effect, the magnetization direction was chosen to be along its length direction under longitudinal vibration, as shown in Fig. 1a.

2.1. Constitutive equations of the laminate composite

Application of H along the length direction of the laminate excites a longitudinal ($d_{33,m}$) mode in the magnetostrictive layer. Two sets of constitutive linearized equations are required to describe the coupled responses of the piezoelectric and magnetostrictive layers. These are [33]

(*Piezoelectric constitutive equation*)

$$\varepsilon_{3p} = s_{33}^{D}\sigma_{3p} + g_{33,p}D_3; \quad E_3 = -g_{33,p}\sigma_{3p} + \beta_{33}^{T}D_3 \tag{2.1.1}$$

(*Piezomagnetism constitutive equations*)

$$\sigma_{3m} = \tfrac{1}{s_{33}^{B}}\varepsilon_{3m} - \lambda_{33}B_3; \quad H_3 = -\lambda_{33}\varepsilon_{3m} + \nu_{33}^{s}B_3 \tag{2.1.2}$$

$$\nu_{33}^{s} = \frac{1}{\mu_{33}^{s}}; \quad \mu_{33}^{s} = \mu_{33}^{T}\left(1 - k_{33,m}^{2}\right);$$

$$s_{33}^{B} = s_{33}^{H}\left(1 - k_{33,m}^{2}\right); \quad k_{33,m}^{2} = \frac{d_{33,m}^{2}}{s_{33}^{H}\mu_{33}^{T}};$$

$$\lambda_{33} = \frac{d_{33,m}}{s_{33}^{H}\mu_{33}^{s}}$$

where ε_{3p} and ε_{3m} are the longitudinal piezoelectric and piezomagnetic strains; D_3 is the dielectric displacement; s_{33}^{D} is the elastic compliance of the piezoelectric material under constant D; $g_{33,p}$ and $d_{33,m}$ are the piezoelectric and piezomagnetic constants; σ_{3p} and σ_{3m} are the longitudinal stresses in the piezoelectric and magnetostrictive layers; β_{33}^{T} is the dielectric stiffness under constant stress;

ν_{33}^s is the magnetic stiffness (reluctivity) under constant strain; μ_{33}^s and μ_{33}^T are the magnetic permeabilities under constant strain and stress; s_{33}^B and s_{33}^H are the elastic compliances of the magnetostrictive layer under constant B_3 and H_3; $k_{33,p}$ and $k_{33,m}$ are the coupling coefficients of the piezoelectric and magnetostrictive layers; λ_{33} is the magnetostrictive coefficient; and B_3 is the magnetization.

Upon considering the insulating layer in the laminate, we have to introduce a third constitutive equation:

$$\varepsilon_{3I} = \frac{1}{Y^I}\sigma_{3I} \tag{2.1.3}$$

where ε_{3p}, σ_{3p} and Y^I are longitudinal strain, stresses and Young's modulus of the insulating layer, respectively.

For Terfenol-D, although strain due to magnetostriction is λH^2, under appropriate magnetic biases pseudo-linear piezomagnetic equations can be used to express their magnetostrictive performances [21, 34]. The optimum magnetic bias will have Terfenol-D working in its optimum magnetostrictive state, but operating in its pseudo-linear piezomagnetic range. In addition, the constitutive equationns. (2.1.1), (2.1.2) and (2.1.3) do not account for loss factors. Significant energy dissipation and nonlinearity in both piezoelectric and magnetostrictive materials are known, in particular under resonant operation. Accordingly, a better analysis would include a mechanical quality factor Q_m to account for dissipation.

2.2. Magneto-elastic-electric coupling

Under an applied H_{ac}, a longitudinal vibration mode is excited by magnetostrictive effect in the Terfenol-D layers of the laminate. Under harmonic motion along $\hat{z}$ (longitudinal direction), it will be supposed that all small mass units Δm_i in the magnetostrictive, piezoelectric and insulation layers of the laminate at z have the same displacement $u(z)$ or strain ε_z, given as

$$u_p(z) = u_m(z) = u_I = u(z)$$

or

$$\varepsilon_{3p}(z) = \varepsilon_{3m}(z) = \varepsilon_{3I} = \varepsilon_3(z) = \frac{\partial u(z)}{\partial z} \tag{2.2.1}$$

This follows from Fig. 1a by assuming that the layers in the laminate act only in a coupled manner, without any sliding between layers. Following Newton's Second Law, we then have

$$\sum_i \Delta m_i \frac{\partial^2 u}{\partial t^2} = \sum_i \sigma_{3i} A_i \tag{2.2.2}$$

where i denotes the layer number, and A_i cross-section area of ith layer. We can then use this motion equation to couple the two piezoelectric and piezomagnetism equations (2.1.1) and (2.1.2).

We have previously derived a solution to the equation of motion for the laminate design shown in Fig. 1 given as

$$u(z) = \frac{\dot{u}_1}{j\omega}\cos kz + \frac{\dot{u}_2 - \dot{u}_1\cos kl}{j\omega \sin kl}\sin kz. \tag{2.2.3}$$

$$k^2 = \frac{\omega^2}{\overline{\upsilon}^2};\ \overline{\upsilon}^2 = \left(\frac{n_m}{s_{33}^B} + \frac{n_p}{s_{33}^D} + n_I Y^I\right)/\overline{\rho}; \tag{2.2.4}$$

where $u(z)$ is the mechanical displacement, $\dot{u}_1$ and $\dot{u}_2$ are the mechanical displacement velocities (i.e., mechanical currents) at the two ends ($z = 0$ and $z = l$) of the laminate; $\bar{\upsilon}$ is the average sound velocity in the laminate; $n_m = \frac{A_m}{A_{lam}}$, $n_p = \frac{A_p}{A_{lam}}$, $n_I = \frac{A_I}{A_{lam}}$ are geometrical factors describing the cross-sectional area ratio (or volume fraction) of the magnetostrictive, piezoelectric and insulation layers, respectively; $A_{lam} = A_m + A_p + A_I$ is cross-sectional area of the laminate; and $\bar{\rho} = n_m\rho_m + n_p\rho_p + n_I\rho_I$ is the average mass density of the laminate. In addition, the forces acting on the end faces of the laminate (at $z = 0$ and $z = l$) can be determined as

$$F_1 = F(0) = -\left(\frac{A_p}{s_{33}^D} + \frac{A_m}{s_{33}^B} + Y^I A_I\right)\frac{\dot{u}_2 - \dot{u}_1\cos kl}{j\bar{\upsilon}\sin kl} + \frac{A_p g_{33,p}}{s_{33}^D}D_3 + \frac{\lambda_{33}}{j\omega N}V_{mag} \tag{2.2.5}$$

$$F_2 = F(l) = -\left(\frac{A_p}{s_{33}^D} + \frac{A_m}{s_{33}^B} + Y^I A_I\right)\frac{\dot{u}_2\cos kl - \dot{u}_1}{j\bar{\upsilon}\sin kl} + \frac{A_p g_{33,p}}{s_{33}^D}D_3 + \frac{\lambda_{33}}{j\omega N}V_{mag}\,. \tag{2.2.6}$$

The strain in the piezoelectric layer caused by the magnetostrictive layers produces a corresponding voltage and current in the piezoelectric one. By eliminating σ in Equation 2.1.1, the electric field across the piezoelectric layers can be determined as

$$E_3 = -\frac{g_{33,p}}{s_{33}^D}\varepsilon_{3,p} + \bar{\beta}_{33}D_3 \tag{2.2.7}$$

where,

$$\bar{\beta}_{33} = \beta_{33}^T\left(1 + \frac{g_{33,p}^2}{s_{33}^D\beta_{33}^T}\right).$$

The output voltage V_{out} produced between the middle and one end of the piezoelectric layer due to the

magnetostrictive strain can then be determined as

$$V_{\text{out1}} = \int_{l/2}^{l} E_3 dz = \frac{-g_{33,\text{p}}}{j\omega s_{33}^D}(\dot{u}_2 - \dot{u}_0) + \bar{\beta}_{33} D_3 l/2$$

or

$$V_{\text{out2}} = \int_{l/2}^{0} -E_3 dz = \frac{g_{33,\text{p}}}{j\omega s_{33}^D}(\dot{u}_1 - \dot{u}_0) - \bar{\beta}_{33} D_3 l/2 \tag{2.2.8}$$

where $\dot{u}_0$ is mechanical displacement velocity at middle point of the laminate. For a λ/2 resonator, the middle is a nodal position, i.e., $\dot{u}_0 = 0$, and $\dot{u}_1 \equiv -\dot{u}_2$. Correspondingly, the induced dielectric displacement current I_{disp1} from one end to the middle or center in one half piezoelectric layer is

$$\text{I}_{\text{disp1}} = \text{j}\omega \text{C}_0 V_{\text{out1}} + \varphi_p(\dot{u}_2 - \dot{u}_0)$$

or

$$I_{\text{disp2}} = -j\omega \text{C}_0 V_{\text{out2}} + \varphi_p(\dot{u}_1 - \dot{u}_0)$$

Because the two output end electrodes of the piezoelectric layer are connected together, and the middle electrode is common ground, the induced current from the whole piezoelectric layer should be

$$\text{I}_{\text{out}} = \text{I}_{\text{disp1}} + (-\text{I}_{\text{disp2}}) = \text{j}\omega(2\text{C}_0)V_{\text{out}} + \varphi_p(\dot{u}_2 - \dot{u}_1)$$

$$C_0 = \frac{A_p}{\bar{\beta}_{33} l/2}, \quad \varphi_p = \frac{A_{\text{p}} g_{33,\text{p}}}{s_{33}^D \bar{\beta}_{33} l/2} \tag{2.2.9}$$

where C_0 is the clamped capacitance, and φ_{p} is elasto-electric coupling factor for the piezoelectric layer.

The forces exerted on the two end faces of the laminate at $z = 0$ and $z = l$ can now be related to the exciting voltage V_{mag}, the mechanical displacement velocities $\dot{u}_1$ and$\dot{u}_2$, and the output voltage V_{out} from the piezoelectric layer, given as

$$F_1 = Z_1 \dot{u}_1 + \left(Z_2 + \frac{\varphi_p^2}{j\omega(-2C_0)}\right)(\dot{u}_1 - \dot{u}_2) + \varphi_{\text{p}} V_{\text{out}} + \varphi_{\text{m}} V_{\text{mag}}$$

$$F_2 = -Z_1 \dot{u}_2 + \left(Z_2 + \frac{\varphi_p^2}{j\omega(-2C_0)}\right)(\dot{u}_1 - \dot{u}_2) + \varphi_p V_{\text{out}} + \varphi_{\text{m}} V_{\text{mag}}$$

$$Z_1 = j\overline{\rho\upsilon} A_{\text{lam}} \cdot tg\left(\frac{kl}{2}\right),$$

$$Z_2 = \frac{\overline{\rho\upsilon} A_{\text{lam}}}{j \sin(kl)}, \quad \varphi_m = \frac{\lambda_{33}}{j\omega N}; \tag{2.2.10}$$

where Z_1 and Z_2 are the mechanical impedances of the laminate; and φ_{m} and φ_{p} are the magneto-elastic and elasto-electric coupling factors. In addition, the input current I_{mag} to coils excites a "mechanical current"$(\dot{u}_1 - \dot{u}_2)$ in the laminate. From Equation 2.1.2b and using Faraday's law, the coupling relation between I_{mag}, V_{mag} and $(\dot{u}_1 - \dot{u}_2)$ can be derived as

$$I_{\text{mag}} = \frac{\lambda_{33}}{j\omega N}(\dot{u}_1 - \dot{u}_2) + \frac{V_{\text{mag}}}{j\omega L^S}$$
$$L^s = Am\mu_{33}^s N^2/l; \tag{2.2.11}$$

where L^s is the clamped inductance, and N is the coils number.

Equations 2.2.9–2.2.11 completely describe the magneto(-elastic-)electric coupling between the magnetostrictive and piezoelectric layers under an exciting current I_{mag} or voltage V_{mag}, via the mechanical displacement velocities $\dot{u}_1$ and $\dot{u}_2$.

2.3. Magnetoelectric equivalent circuit under resonance drive

Based upon the magnetoelectric coupling equations 2.2.9–2.2.11, a magnetoelectric equivalent circuit can be derived for the longitudinal vibration mode of the geometry shown in Fig. 1. This equivalent circuit is shown in Fig. 2a.

Under free boundary conditions, the force acting on the end faces are $F_1 = 0$ and $F_2 = 0$. Thus, we can short the two channels to ground. Under this condition, the circuit of Fig. 2a is simplified to that shown in Fig. 2b. Note that Z in the Fig. 2b is: $Z = \overline{\rho\upsilon} A_{\text{lam}}/j2\tan(kl/2)$. In this simplified circuit, the input current I_{mag} (or voltage V_{mag}) excites a "mechanical current"$I_c = \dot{u}_1 - \dot{u}_2$, via the magneto-elastic coupling factor ϕ_{m}. Subsequently, I_{c} induces an output voltage V_{out}, via the elasto-electric coupling.

Assuming the laminate composite to be a λ/2-resonator, operating in a length extensional mode, the series angular resonance frequency is $\omega_s = \frac{\pi\bar{\upsilon}}{l}$. Under resonant drive the mechanical impedance Z in the equivalent circuit of Fig. 2b can be approximated by a Taylor series expansion of the frequency $f(\omega)$ about ω_{s}, given as

$$f(\omega) = \frac{Z_0}{j2\tan\frac{\omega l}{2\bar{\upsilon}}} = f(\omega_s) + f'(\omega_s)(\omega - \omega_s) + \frac{1}{2}f''(\omega_s)(\omega - \omega_s)^2 + \ldots \approx -\frac{\pi Z_0}{4j\omega_s}(\omega - \omega_s)$$
$$= -2jL_{\text{m}}(\omega - \omega_s) \tag{2.3.1}$$

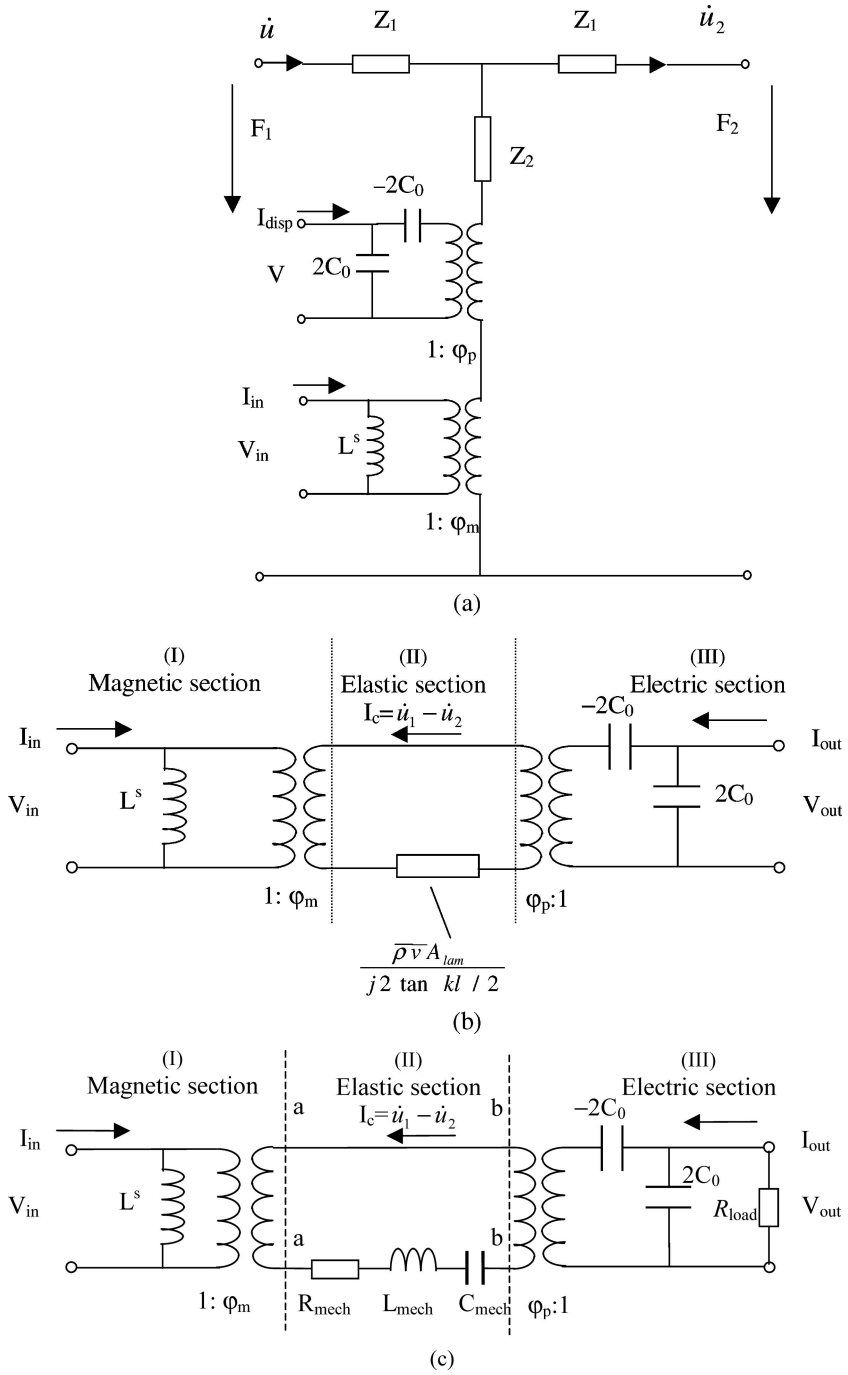

Figure 2 Magnetoelectric equivalent circuits. (a) Magnetoelectric equivalent circuit for a longitudinal-extension vibration mode under applied ac voltage V_{in} and (b) under free-free boundary condition, and (c) under resonance drive with load R_{Load}.

Then, compared with the impedance expansion of a series L_m, C_m circuit, we finally obtain

$$\omega_s^2 = \frac{1}{L_{mech}C_{mech}}; \quad L_{mech} = \frac{\pi Z_0}{8\omega_s};$$
$$C_{mech} = \frac{1}{\omega_s^2 L_{mech}}; \quad Z_0 = \overline{\rho v} A_{lam} \qquad (2.3.2)$$

where L_{mech} and C_{mech} are the motional mechanical inductance and capacitance.

At resonance, this equation yields an approximation for the mechanical impedance Z. The mechanical quality factor Q_m of the laminate under resonance drive is finite, due to dissipation [35]. This limitation of the vibration amplitude must also be included, in order to accurately predict the resonant response. Finite values of Q_{mech} result

in an effective motional mechanical resistance R_{mech} of

$$R_{\text{mech}} = \frac{\omega_s L_{\text{mech}}}{Q_{\text{mech}}} = \frac{\pi Z_0}{8 Q_{\text{mech}}}. \tag{2.3.3}$$

Accordingly, the equivalent circuit of the laminate under resonance drive is given in Fig. 2c, where R_{Load} is an external load.

3. Calculating results and discussion

3.1. Magnetoelectric coupling

The magnetoelectric coupling effect is a product property between the magneto-elastic and elasto-electric coupling coefficients. We can define the effective magnetoelectric coupling $k_{\text{mag-elec}}$ (eff) in terms of energy (U) as

$$k^2_{\text{mag-elastic}}(\text{eff}) \equiv \frac{U^{\text{out}}_{\text{electrical}}}{U^{\text{stored}}_{\text{elastic}}} \times \frac{U^{\text{stored}}_{\text{elastic}}}{U^{\text{input}}_{\text{magnetic}}}$$
$$\approx k^2_{\text{mag-elastic}}\,(\text{eff}) \times k^2_{\text{elasto-elec}}\,(\text{eff}) \tag{3.1.1}$$

where $k_{\text{mag-elastic}}$ (eff) and $k_{\text{elasto-elec}}$ (eff) are the magneto-elastic and elasto-electric coupling factors.

3.1.1. Efffective magneto-elastic coupling factor

By setting the elasto-electric coupling factor φ_{p} to zero (i.e., no piezoelectric phase), the laminate shown in Fig.1a becomes a magneto-elastic transducer or resonator. From Fig. 2c, the magnetic-elastic coupling factor is then given as [34]

$$k^2_{\text{mag-elastic}}\,(\text{eff}) = \frac{\omega_p^2 - \omega_s^2}{\omega_p^2}; \tag{3.1.2}$$

where ω_{p} and ω_{s} are parallel resonance and series resonance frequencies of the magneto-elastic resonator with infinite Q_{mech} and zero load. From the circuit in Fig. 2c (b-b in short circuit), ω_{p} and ω_{s} can be related to the input admittance Y_{e}, as

$$Y_e = \frac{1}{j\omega L^s} + \frac{\varphi^2_{\text{m}}}{R_{\text{mech}} + j\omega L_{\text{mech}} + \frac{1}{j\omega C_{\text{mech}}}}. \tag{3.1.3}$$

At resonance, the input admittance Y_{e} is purely resistive, i.e, $Y_{e(\text{imaginary})} = 0$ for $R_{\text{mech}} = 0$. This gives $\omega_s^2 = \frac{1}{L_{\text{mech}}C_{\text{mech}}}$ and $\omega_p^2 = \frac{1}{L_{\text{mech}}}(\frac{1}{C_{\text{mech}}} + \frac{k^2_{33,m}}{C^B})$. Following equation (3.1.2), we obtain the magneto-elastic coupling factor as

$$k^2_{\text{mag-elastic}}\,(\text{eff}) = \frac{C_{\text{mech}}}{C^B + C_{\text{mech}} k^2_{33,\text{m}}} k^2_{33,\text{m}} \tag{3.1.4}$$

where $C^B = (1 - k^2_{33,\text{m}})C^{\text{H}}$ is the elastic compliance of the magnetostrictive layers at constant B, and $C^{\text{H}} = \frac{l s^{\text{H}}_{33}}{A_m}$ is the compliance at constant H.

3.1.2. Effective elasto-electric coupling factor

To obtain $k^2_{\text{elasto-electric}}$ (eff), the magnetic section of the equivalent circuit is electrically shorted (i.e., $\phi_{\text{m}} = 0$, and a-a is shorted in Fig. 2c). Thus, the magnetoelectric equivalent circuit becomes the standard equivalent circuit of a piezoelectric resonator, near its resonance frequency ω_{r}. The electromechanical coupling is [33]

$$k_{\text{elasto-electric}}\,(\text{eff}) = \frac{\omega_p^2 - \omega_s^2}{\omega_p^2}; \tag{3.1.5}$$

where ω_{p} and ω_{s} are parallel resonance and series resonance frequencies of the elastic-electric vibrator with infinite Q_{mech} and zero external load. From the circuit in Fig. 2c, ω_{p} and ω_{s} can be related to the output admittance Y_{o}, as

$$Y_o = j\omega(2C_0) + \frac{\varphi_p^2}{R_{\text{mech}} + j\omega L_{\text{mech}} + \frac{1}{j\omega C'_{\text{mech}}}}; \tag{3.1.6}$$

where ω_{p} and ω_{s} can be obtained as $\omega_r^2 = \frac{1}{L_{\text{mech}}C_{\text{mech}}}$ and $\omega_s^2 = \frac{1}{L_{\text{mech}}C'_{\text{mech}}}$; and$C'_{\text{mech}} = \frac{C_{\text{mech}}\cdot(2C_0)}{(2C_0) - C_{\text{mech}}\varphi_p^2}$. Thus, the effective elasto-electric coupling factor is

$$k^2_{\text{elasto-electric}}\,(\text{eff}) = \frac{C_{\text{mech}}\varphi_p^2}{2C_0}. \tag{3.1.7}$$

3.1.3. Effective magneto-electric coupling factor

The effective magnetoelectric coupling factor $k_{\text{mag-elec}}$(eff) can now be obtained by inserting equations (3.1.4) and (3.1.7) into (3.1.1), and simplifying to

$$k^2_{\text{mag-elec}}\,(\text{eff}) = \frac{64 s^B_{33} k^2_{33,\text{m}} g^2_{33\text{p}} n_{\text{m}} n_{\text{p}}}{\pi^2 \bar{\beta}_{33}\left(n_{\text{m}} s^D_{33} + n_{\text{p}} s^B_{33} + n_I Y^I s^B_{33} s^D_{33}\right)[\pi^2/2\left(n_{\text{m}} s^D_{33} + n_p s^B_{33} + n_I Y^I s^B_{33} s^D_{33}\right) + 8 n_{\text{m}} k^2_{33\text{m}} s^D_{33}]}$$

$$s^B_{33} = s^H_{33}\left(1 - k^2_{33,m}\right),\ s^D_{33} = s^E_{33}\left(1 - k^2_{33,p}\right) \tag{3.1.8}$$

If $n_{\text{m}} = 0$ or $n_{\text{p}} = 0$, then $k^2_{\text{mag-elec}}$(eff) $= 0$. Thus, there is an optimum geometric parameter n_{opt} at which$k^2_{\text{mag-elec}}$(eff) is maximum. This occurs at$\frac{\partial k^2_{\text{mag-elec}}(\text{eff})}{\partial n_m} = 0$ (or$\frac{\partial k^2_{\text{mag-elec}}(\text{eff})}{\partial n_p} = 0$). Assuming the

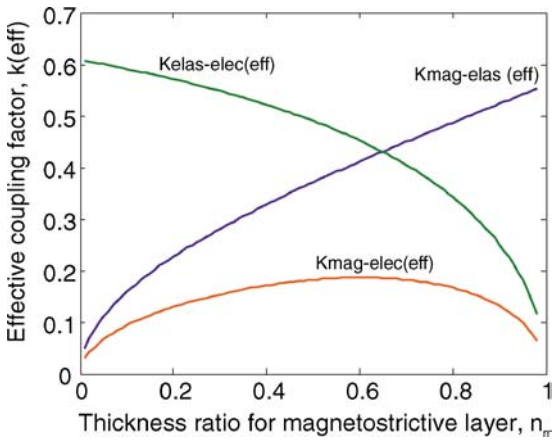

Figure 3 Effective magneto-elastic ($K_{\text{mag-elas, eff}}$), elasto-electric ($K_{\text{elas-elec, eff}}$), and magnetoelectric coupling factors ($K_{\text{mag-elec, eff}}$).

insulating layer to be thin, the optimum geometric parameter for the magnetostrictive layer is then

$$n_{\text{m,opt}} = \frac{1}{1+\gamma(1+8k_{33m}^2/\pi^2)^{1/2}} \tag{3.1.9}$$

where $\gamma = \frac{s_{33}^D}{s_{33}^B}$ is a ratio of the compliance constants of the piezoelectric and magnetostrictive layers.

Fig. 3 shows a calculation of $k_{\text{mag-elec}}$ (eff) as a function of the geometric parameter n_{m} for a laminate of piezoelectric PZT-8 (APC-841) and magnetostrictive Terfenol-D. When $n_{\text{m}} = 0$, this laminate composite contains no magnetostrictive material, thus$k_{\text{mag-elec}}$ (eff) is zero. Correspondingly, when $n_{\text{m}} = 1$, the laminate contains only magnetostrictive material, and again$k_{\text{mag-elec}}$ (eff) is zero. Between these two geometric limits, a maximum value of$k_{\text{mag-elec}}$ (eff) ~ 0.2 is found, as can be seen in Fig. 3 near $n_{\text{m}} \sim 0.61$.

3.2. Magnetoelectric voltage gain under resonance drive

A magnetoelectric voltage gain was found by analysis of the equivalent circuit in Fig. 2c. Assuming that the circuit is unloaded and by applying Ohm's law to the mechanical loop (elastic section), the voltage gain ($V_{\text{out}}/V_{\text{in}}$, and $V_{\text{in}} = V_{\text{mag}}$) can be estimated as

$$\frac{\varphi_p V_{\text{out}}}{\varphi_m V_{\text{in}}} = \left| \frac{\varphi_p^2/j\omega(2C_0)}{R_m + j\omega L_m + 1/j\omega C_m + 1/j\omega(-2C_0) + 1/j\omega(2C_0)} \right|$$

or

$$\frac{V_{\text{out}}}{V_{\text{in}}} = \left| \frac{\varphi_p\varphi_m}{j\omega(2C_0)} \frac{1}{R_m + j\omega L_m + 1/j\omega C_m} \right| \tag{3.1.11}$$

Under resonant drive, where $\omega_s = \left(1/L_{\text{mech}}C_{\text{mech}}\right)^{1/2}$, the maximum voltage gain V_{gain1} is

$$V_{\text{gain1,max}} = \frac{4Q_{\text{mech}}\varphi_m\varphi_p}{\pi\omega_s C_0 Z_0}. \tag{3.1.12}$$

From this relationship, it can be seen that the maximum voltage gain is strongly dependent on mechanical quality factor Q_{m}. Calculations for a Terfenol-D/PZT laminate composite based on Equation 3.1.11 show that the maximum voltage gains at resonance are 1.54×10^5 for $Q_{\text{m}} = 1000$, 1.55×10^4 for $Q_{\text{m}} = 100$, and 7.7×10^3 for $Q_{\text{m}} = 50$, respectively. These calculated values are far higher than experimental data.

However, we can further simplify the equivalent circuit from Fig. 2c into Fig. 4a, and it can be seen that the ratio of output voltage to input voltage (voltage gain V_{gain2}) is proportional to the impedance ratio (according to Ohm's Law). Thus, the modified voltage gain is

$$V_{\text{gain2}} = \left|\frac{V_{\text{out}}}{V_{\text{in}}}\right| = \alpha \left| \frac{\dfrac{1}{j\omega C}}{R_1 + j\omega L_1 + \dfrac{1}{j\omega C_1} + \dfrac{1}{j\omega C}} \right| \tag{3.1.13}$$

where $C = C_0\varphi_m^2/2\varphi_p^2; R_1 = R_{\text{mech}}/\varphi_m^2; L_1 = L_{\text{mech}}/\varphi_{\text{m}}^2; C_1 = \varphi_{\text{m}}^2 C'_{\text{mech}}.\alpha$ is a dimensionless ratio factor, relating dc magnetic bias. If we choice $\alpha = 1$, the maximum voltage gain V_{gain2} under resonance drive is

$$V_{\text{gain2,max}} = \frac{4Q_{\text{mech}}\varphi_p^2}{\pi\omega_s C_0 Z_0} \tag{3.1.14}$$

From this relationship, it can be seen that the maximum voltage gain is mainly related to the piezoelectric section of the equivalent circuit in Fig. 4a. The voltage gain is directly proportional to Q_{mech} and $\phi_{\text{p}}{}^2$ (or $g_{33,\text{p}}^2$) in piezoelectric layer. This is because the output voltage is generated by this section. The function of the magnetic section of the circuit is to transducer the magnetic energy into a mechanical vibration. The piezoelectric one subsequently transduces this vibration to an electric output.

Fig. 4b shows the calculated voltage gain V_{gain} as a function of frequency for $Q_{\text{m}} = 100, 500$ and 1400. These calculations were performed using Equations 3.1.11 and

3.1.13, assuming a Terfenol-D/PZT laminate length of 70 mm, width of 10 mm, and thickness of 6 mm. The voltage gain for $Q_m = 100$ was only ~20. However, for $Q_{mech} = 500$, the gain was ~100. A typical value of Q_{mech} for PZT-8 is 1400; using this value, a maximum voltage gain of 280 can be estimated. Calculation values using Equation 3.1.13 are much close to our measured voltage gain ones.

This voltage gain is significantly larger than that of other voltage gain devices, such as electromagnetic and piezoelectric transformers [36, 37]. The ME voltage gain effect is quite purposeful for power electronics, such as transformer application.

3.3. Efficiency

To estimate the efficiency of magnetoelectric transduction, the equivalent circuit in Fig. 4a was converted by an impedance method to that shown in Fig. 5a. In so doing, it was assumed that the losses in the laminate are only mechanical, i.e., electrical losses (eddy current loss) were neglected. Assuming a load of Z_{Load}, the magnetoelectric efficiency of the laminate at resonance is

$$\eta = \frac{P_{out}}{P_{in}} = \frac{I^2 \cdot \mathrm{Re}(Z_{Load})}{I^2 \cdot \mathrm{Re}(Z_{in})} = \frac{R_{Load}}{R_{Load} + (\varphi_m/\varphi_p)^2[1 + (2\omega_s C_0 R_{Load})^2]R_1}. \quad (3.1.15)$$

By setting $\delta\eta/\delta R_{Load} = 0$, the optimum load can be estimated as $R_{Load,opt} = \frac{1}{2\omega_s C_0}$. When $R_{Load} = R_{Load,\ opt}$, the circuit has maximum output power. Under resonant operation, the maximum efficiency is given as $\eta_{max} = \frac{\varphi_p^2}{\varphi_p^2 + \frac{\pi Z_0 C_0 \omega_s}{Q_{mech}}}$. Clearly, a higher Q_{mech} results in a higher transduction efficiency.

Fig. 5b shows the calculated value of η as a function of R_{Load} for different values of Q_m. η can be seen to vary significantly with R_{Load}. A maximum efficiency η_{max} was found for $R_{Load} \approx 2 \times 10^6$ ohms. The value of η_{max} at this R_{Load} is dependent on Q_m. For $Q_m = 100$, η_{max} was less than 90%; however, for $Q_{mech} = 1000$, η_{max} was ≈98%. However, for a bulk Terfenol-D material operated of a

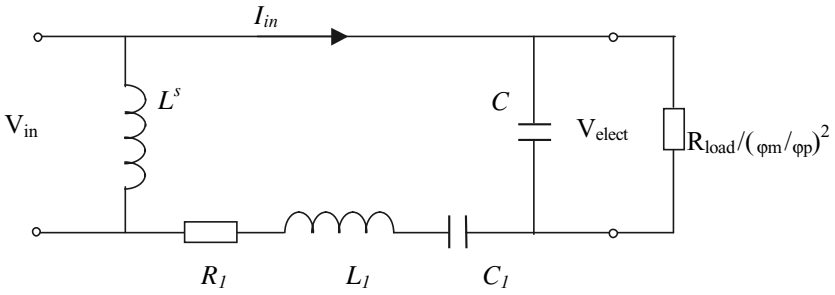

(a)

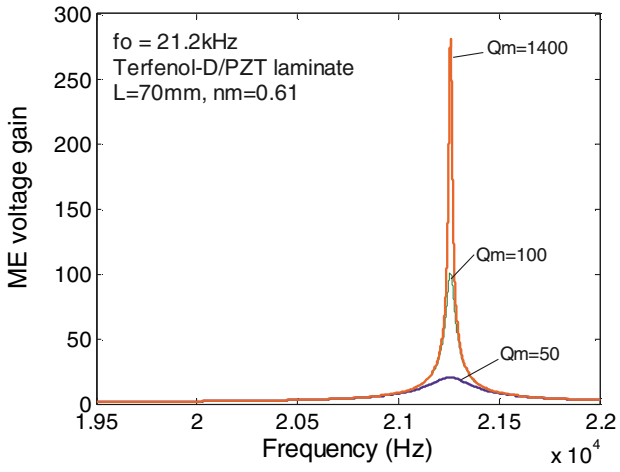

(b)

Figure 4 Simplified equivalent circuit and voltage gain calculated using Equation 3.1.13. (a) Equivalent circuit, and (b) calculated voltage gain.

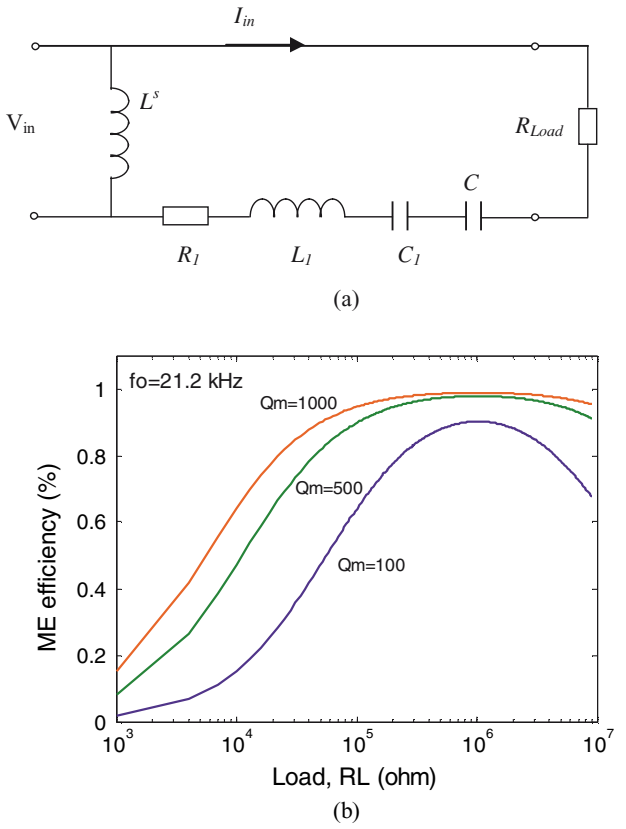

Figure 5 Simplified equivalent circuit illustrating magnetoelectric efficiency, and magnetoelectric efficiency calculated using equation 3.1.15. (a) Equivalent circuit, and (b) calculated efficiency. (Eddy current effects and electric loss in stored energy elements, L^s, C_1 and C', are neglected). In Fig.5a, $R'_{\text{Load}} = \frac{R_{\text{Load}}}{[1+(2\omega C_0 R_{\text{Load}})^2](\varphi_m/\varphi_p)^2}$; $C' = \frac{[1+(2\omega C_0 R_{\text{Load}})^2]}{\omega^2(2C_0)^2 R_{\text{Load}}^2}(\frac{\varphi_m}{\varphi_p})^2(2C_0)$.

high frequency of >20 kHz, the eddy current losses will be serious, resulting in that the effective magnetoelectric efficiency far lower than the theoretical value. To overcome the eddy current losses, a thin multi-layer design is necessary for high-power magnetoelectric transformer applications.

4. Experiments

We designed and fabricated one long-type of Terfenol-D/PZT magneto-electric laminates with dimensions of 70 mm in length, 10 mm in width, and 6 mm in thickness. The Terfenol-D layers were grain-oriented in the length direction, and the PZT layer (PZT-8) was polarized in length direction too. The PZT plate was laminated between two Terfenol-D plates and insulated with thin glass layers using an epoxy resin, and cured at 80°C for 3–4 h under load. The induced voltages across the two electrodes of PZT layer under a drive by coils around the laminate were then measured using an oscilloscope. Fig. 6 shows the measured voltage gain, the ratio of induced voltage V_{out} to inputted voltage V_{in} to coils, of our ME transformer as a function of the drive frequency f. A maximum voltage gain of ~260 was found at a resonance frequency of 21.3 kHz. In addition, at the resonance state, the maximum voltage gain of the ME transformer was strongly dependent on an applied dc magnetic bias H_{dc}. For H_{dc}≈300 Oe, our prototype exhibited a maximum voltage gain of ≈300, which is quite close to the predicted value using (3.1.14).

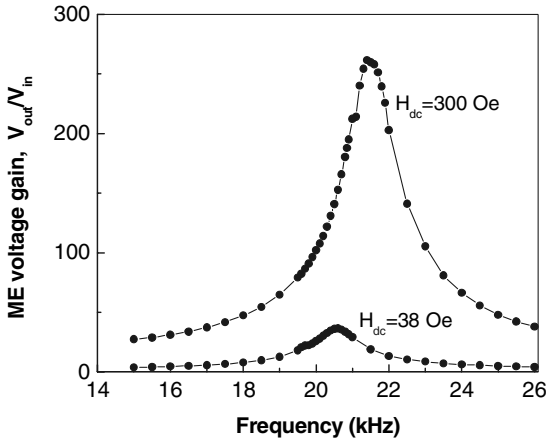

Figure 6 Measured magneto-electric voltage gain effect under resonance drive.

Compared with conventional electromagnetic transformers, our ME transformer (i) does not require secondary coils with a high-turns ratio in order to obtain a step-up voltage output; and (ii) it has significantly higher voltage gains and a notably wider frequency bandwidth due to low Q_{m} of Terfenol-D materials. For example, the voltage gain and frequency bandwidth for a typical piezoelectric transformer are only 10–100 and 0.1 kHz [36, 37], which are far lower than the 300 and 1.5 kHz observed for our ME transformer, respectively.

5. Summary

Effective magneotelectric couplings, output efficiencies and voltage gains have been analyzed based on a ME equivalent circuit method for laminate composites of piezoelectric PZT and magnetostrictive Terfenol-D. The analysis predicts: (i) there is an optimum geometric parameter n_{opt} which maximizes $k_{\text{mag-elec}}$ (eff); (ii) a high voltage gain occurs under resonance drive, exceeding values of 280 for $Q_{\text{mech}} = 1400$; (iii) a maximum efficiency occurs when the external load equals the impedance of the static capacitance, η_{max}~98% for $Q_{\text{mech}} = 1000$ for a multi-thin-layer design; and (iv) higher values of Q_{mech} in piezoelectric material result in higher voltage gains and maximum efficiencies. Our experimental results confirm that the ME laminate has a strong voltage gain effect. This is an important finding, as there are many potential applications for high-power solid-state ME transformers.

Acknowledgments

This research was supported by the Office of Naval Research under grants N000140210340, N000140210126, and MURI N000140110761.

References

1. L. D. LANDAU and E. LIFTSHITZ, "Electrodynamics of Continuous Media" (Pergamon Press, Oxford, 1960) P.119.
2. DI MATTEO and S. JANSEN, AGM, *Phys. Rev. B* **66** (2002) 100402.
3. I. E. DZYALOSHINSKII, *Sovit Phys.*-JETP **37** (1959) 81 [*Sov. Phys JETP* **10** (1960) 628].
4. L. WIEGELMANN, A. A. STEPANOV, I. M. VITEBSKY, A. G. M. JANSEN and P. WYDER, *Phys. Rev. B* **49** (1994) 10039.
5. J. WANG, J. B. NEATON, H. ZHENG, V. NAGARAJAN, S. B. OGALE, B. LIU, D. VIEHLAND, V. VAITHYANATHAN, D. G. SCHLOM, U. V. WAGHMARE, N. A. SPALDIN, K. M. RABE, M. WUTTIG and R. RAMESH, *Sci.* **299** (2003) 1719.
6. J. RYU, A. VAZQUEZ-ARAZO, K. UCHINO and H. KIM, *J. Electro.* **7** (2001) 17.
7. T. WU and J. HUANG, *International J. of Solids and Strus.* **37** (2000) 2981.
8. C. NAN, M. LI and J. HUANG, *Phys. Review B* **63** (2001) 144415. C. NAN, *Phys. Rev. B.* **50** (1994) 6082.
9. C. NAN, N. CAI, Z. SHI, J. ZHAI, G. LIU and Y. LIN, *ibid.* **71** (2005) 014102.
10. M. BICHURIN, D. A. FILIPPOV and V. M. PETROV, *ibid.* **68** (2003) 132408.
11. S. X. DONG, J. CHENG, J.F. LI and D. VIEHLAND, *Appl. Phys. Lett.* **83** (2003) 4812.
12. H. YU, M. ZENG Y. WANG, *et al., ibid.* **86** (2005) 032508.
13. M. ZENG, J.G. WAN, Y. WANG, *et al. J. Appl. Phys.* **95** (2004) 8069.
14. D. A. FILIPPOV, M. BICHURIN, V. PETROV, *et al., Phys. Solid State* **46** (2004) 1674.
15. S. X. DONG, J. F. LI and D. VIEHLAND, *Appl. Phys. Lett.* **85** (2004) 5305.
16. *Idem., ibid.*, **85** (2004) 3534.
17. *Idem., ibid.* **84** (2004) 4188.
18. M. AVELLANEDA and G. HARSHE, *J. Inte. Mate. Systems and Struc.* **5** 501 (1994).
19. J. RYU, A. VAZQUEZ-ARAZO, K. UCHINO and H. KIM, *Jpn. J. Appl. Phys.* **40** (2001) 4948.
20. G. SRINIVASAN, E. RASMUSSEN, B. LEVIN and R. HAYES, *Phys. Rev. B* **65** (2002) 134402.
21. G. SRINIVASAN, E. RASMUSSEN, J. GALLEGOS, R. SRINIVASAN, Y. BOKHAN and V. LALETIN, *ibid. B* **64** (2001) 214408.
22. J. RYU, S. PRIYA, A. VAZQUEZ-ARAZO, K. UCHINO and H. KIM, *J. Am. Ceram. Soc.* **84** (2001) 2905.
23. G. SRINIVASAN, V. LALETIN, R. HAYES, N. PUDDUBNAYA, E. RASMUSSEN and D. FEKEL, *Solid State Commu.* **124** (2002) 373.
24. M. BICHURIN, V. PETROV and G. SRINIVASAN, *J. Appl. Phys.* **92** (2002) 7681.
25. K. MORI and M. WUTTIG, *Appl. Phys. Lett.* **81** (2002) 100.
26. S. X. DONG, J.F. LI and D. VIEHLAND, *IEEE Transactions on Ultrasonics, Ferroelectrics, and Freque. Control* **50**(1) (2003) 253.
27. *Idem., J. Appl. Phys.* **96** (2004) 3382.
28. S. X. DONG, J. ZHAI, Z. XING, J.F. LI and D. VIEHLAND, *Appl. Phys. Lett.* **86** (2005) 102901.
29. S. X. DONG, J.F. LI and D. VIEHLAND, *ibid.* **85** (2004) 2307.
30. *Idem., IEEE Transactions on Ultrasonics, Ferroelectrics, and Frequency Control* **50** (2003) 1236.
31. *Idem., ibid.* **51** (2004) 794.
32. Idem., *J. Appl. Phys.* **97** (2005) 103902.
33. W. MASON, "Physical Acoustics, Principle and Methods" (New York Academic Press 1964) p. 263.
34. G. ENGDAHL, "Magnetostrictive Materials Handbook" (Academic Press, ISBN: 0-12-238640-X, 2000).
35. W. G. CADY, "Piezoelectricity, An Introduction to theory and applications of Electromechanical Phenomena in Crystal" (Dover Publications, New York, 1964).
36. A. VAZQUEZ-CARAZO, in Fifth International Conference on Intelligent Materials (Smart System and Nanotechnology, University Park, PA, USA 2003).
37. C. ROSEN, "Elect. Components Symposium," 7th (Washington, D.C., 1956) p.205.